Hindawi
Advances in Civil Engineering
Volume 2018, Article ID 9327528, 9 pages
https://doi.org/10.1155/2018/9327528

Research Article

Evaluation of Methods to Correct the Effect of Temperature on Electrical Conductivity of Mortar

Milena Rangelov[1] and Somayeh Nassiri[2]

[1]*Postdoctoral Fellow, Washington State University, 2001 East Grimes Way, PACCAR, Pullman, WA 99164-5815, USA*
[2]*Assistant Professor, Washington State University, 2001 East Grimes Way, 248 PACCAR, Pullman, WA 99164-5815, USA*

Correspondence should be addressed to Somayeh Nassiri; snassiri@wsu.edu

Received 26 September 2018; Accepted 22 November 2018; Published 13 December 2018

Academic Editor: Xu Yang

Nondestructive methods to obtain the electrical conductivity (σ) or resistivity (ρ) of concrete are gaining popularity for durability evaluation. However, these methods are susceptible to the effects of curing and conditioning, primarily temperature and degree of saturation. Before σ of concrete at varied temperatures can be used for durability assessment, appropriate corrections must be made to account for the effect of temperature (T). In this study, two existing and one new temperature correction methods were evaluated for 12 mortar mixtures varying in water-to-cementitious material ratio (w/cm) and the content and types of supplementary cementitious materials (SCM). Mortar specimens instrumented with embedded sensors were cured in sealed conditions for 11–13 months. After this period, the sealed specimens were subjected to stepwise temperature change in 5–50°C range while σ was recorded using the embedded sensors. Linear, bilinear, and Arrhenius temperature correction (LTC, BLTC, and ATC, respectively) were fitted to the obtained σ-T datasets and were evaluated for fitness. LTC provided an acceptable fit to the σ-T data ($R^2 > 0.81$) but was found the most suitable in 5–30°C temperature range. BLTC was defined as a combination of two distinct LTC below and above the reference temperature at 23°C and had a better fit to the data ($R^2 > 0.96$). Lastly, ATC showed the best fit among the tested methods ($R^2 > 0.98$) and was found applicable for the full tested temperature range. Comparison of correction coefficients among the mixtures indicated that increase in w/cm results in less sensitivity of σ to temperature. Mixtures with SCM generally exhibit higher temperature sensitivity compared to the corresponding plain mixture. Since the variations in correction coefficients were not substantial (less 18% variation among 10 of 12 mixtures), a single value of activation energy of conduction (E_c) at 32 kJ/mol was identified as the general recommendation for all the tested mixtures.

1. Introduction

In recent years, nondestructive techniques for indirect assessment of concrete transport properties and durability by measuring electrical conductivity (σ) or resistivity (ρ) have gained popularity [1]. The measurements are taken by several available methods based on uniaxial or bulk resistivity, surface resistivity, electrical impedance spectroscopy, and noncontact resistivity measurements based on the transformer principle [1–5]. Additionally, embedded sensors for real-time ρ monitoring were evaluated in past studies [6–8]. Since electrical current in the concrete is primarily conducted through the pore solution in the pore system, electrical measurements can be used to indirectly evaluate pore system and transport properties of concrete [5, 6, 9, 10]. Relatively high ρ (low σ) is a characteristic of concrete with dense microstructure, low porosity, and poorly interconnected pores. This type of microstructure hinders the ingress of water and ions that typically leads to durability-related distresses. In several research studies, σ or ρ were utilized to evaluate chloride diffusivity or permeability, which is a key input for service life predictions of reinforced concrete structures exposed to chlorides [7,11–13]. Due to simplicity, rapid nature, and nondestructive nature of the data collection, as well as availability of commercial apparatus, electrical methods are becoming more common in concrete durability evaluation [14, 15].

Despite the convenience of these methods, data interpretation still requires more research as multiple factors, such as mixture design, temperature, and degree of saturation, have combined influences on the results [1, 16]. The synergistic effect of these factors should be taken into consideration when interpreting σ or ρ data in cementitious systems. The focus of this study is the effect of temperature and evaluation of existing correction methods.

Changes in temperature (T) induce changes in the ionic mobility, pore solution concentration, and ion-to-ion and ion-to-solids interactions in the pore solution, which result in changes in the overall conductivity of the concrete [14]. Since accurate assessment of these effects is complex and difficult, the effect of temperature on σ is typically evaluated empirically. The simplest type of σ-T dependency investigated in the literature is linear, typically defined through linear temperature correction (LTC) [8,17–19]:

$$\frac{\sigma}{\sigma_{\text{ref}}} = \frac{\rho_{\text{ref}}}{\rho} = \frac{(T_c - T_{\text{ref}})\alpha}{100} + 1, \tag{1}$$

where T_{ref} is the reference temperature in °C, typically defined in a value in the 21–25°C range, ρ_{ref} and σ_{ref} are the resistivity and conductivity at T_{ref}, T_c is the conditioning temperature in °C, and α is a linear correction coefficient (%/°C). The recommended values of α range from 3 to 5% per 1°C temperature increase [17–19]. However, LTC was found effective only in a small temperature range (±5°C of the reference temperature) [20].

In addition to LTC, the Arrhenius form equation was used in the literature for temperature correction (hereafter: ATC) [3, 8, 16, 17, 20, 21]:

$$\frac{\sigma}{\sigma_{\text{ref}}} = \frac{\rho_{\text{ref}}}{\rho} = \exp\left[-\frac{E_c}{R}\left(\frac{1}{T_c + 273} + \frac{1}{T_{\text{ref}} + 273}\right)\right], \tag{2}$$

where R is the universal gas constant (8.314 J/molK) and E_c is the activation energy of conduction in kJ/mol. Higher values of correction coefficients (α and E_c for LTC and ATC, respectively) indicate higher temperature sensitivity of the mixture [17]. Typical values of E_c from the literature range from 12.54 to 42.47 kJ/mol and primarily depend on the degree of saturation, with sealed specimens presenting higher E_c compared to the saturated ones [3, 8, 16, 17, 20, 21].

Spragg et al. compared temperature correction of ρ for saturated concrete specimens measured by the uniaxial versus the surface resistivity method and found that surface resistivity method yields E_c that are 7 to 15% higher than that by the uniaxial method [16]. The identified difference in E_c was attributed to the effects of leaching occurring on the surface of the specimen detected by surface resistivity meter [16]. Weiss et al. evaluated the LTC and ATC methods for 13 concrete mixtures varying in water-to-cementitious materials ratio (w/cm) and binder type (Portland cement, binary, and ternary mixtures) for $5 < T_c < 30$°C by uniaxial resistivity method [17]. Saturated specimens were found to be less sensitive to temperature (smaller values of α and E_c) compared to their sealed counterparts, and both LTC and ATC were found satisfactory. However, due to higher temperature sensitivity of the sealed specimens, ATC was recommended as the reliable temperature correction method [17].

As reviewed above, the effectiveness of various temperature correction methods was evaluated in only one study. The suitability of current methods at higher temperatures (30–50°C) which is representative of in-service conditions in hot climate areas is yet to be evaluated. Further, the effect of mixture parameters and SCMs on temperature sensitivity of mixes requires more investigation. The effectiveness of the correction methods for data collection methods other than uniaxial resistivity method deserves further research. Currently, the electrical characterization methods are mostly limited to laboratory conditions, whereas the appropriate durability characterization would require real-time in situ durability assessment. This can be achieved by the use of embedded electrical sensors; however, appropriate corrections for environmental conditions have to be applied. So, this study puts forward a framework for temperature corrections of sensor-based σ, which is a necessary step for in situ durability evaluation.

In this study, sensor-based σ data are used from a variety of mortar mixtures over a wide temperature range from 5 to 50°C to investigate the effectiveness of both the LTC and ATC methods. Temperature sensitivity of mixes containing varied w/cm and contents of ground granulated blast furnace slag (GGBFS), class F fly ash, and silica fume is investigated. Recommended values for the correction parameters of each method are developed based on the tested mixtures.

2. Description of Experiment

2.1. Materials and Mixtures. The experimental matrix included 12 mortar mixture designs with proportioning listed in Table 1. Implemented aggregate was river sand with specific gravity 2.51 and fineness modulus 3.06. A reference mixture (control) was prepared with ordinary type I/II Portland cement, w/cm of 0.45, and aggregate-to-binder ratio of 1.95. The remaining 11 test mixtures had the same aggregate-to-binder ratio as the control but varied in water content and cementitious materials as follows:

(i) W mixtures with varied w/cm at 0.35, 0.40, and 0.50

(ii) GGBFS mixtures with partial cement replacement by GGBFS at 20 and 40 percent by mass (GGBFS_20, GGBFS_40)

(iii) Fly_ash mixtures with partial cement replacement by class F fly ash at 20, 40, and 60 percent by mass (Fly_ash_20, Fly_ash_40, Fly_ash_60)

(iv) S_fume mixtures with partial cement replacement by class silica fume at 5, 10, and 15 percent by mass (S_fume_5, S_fume_10, S_fume_15)

Chemical composition of cementitious materials used in the study is provided in Table 2.

2.2. Specimen Casting and Instrumentation. Mortar mixtures specified in Table 1 were prepared following ASTM C305 [22]. One Φ100 by 200 mm cylindrical specimen per mixture

Table 1: Mortar constituents and their proportioning for the mixtures used in the study.

Mixture group	Constituent content (kg/m^3)					w/cm
	Fine aggregate	Ordinary type I/II Portland cement	Class F fly ash	GGBFS	Silica fume	
Control (W0.45, Fly_ash_0, GGBFS_0, S_fume_0)	1,291.0	662.8	0	0	0	0.45
W Mixes	W0.35, W0.40, and W0.50 with w/cm = 0.35, 0.40, and 0.50					
GGBFS mixes	GGBFS_20 and 40 with GGBFS % = 20 and 40; w/cm = 0.45					
Fly_ash mixes	Fly_ash_20, 40, 60 with fly ash % = 20, 40, and 60; w/cm = 0.45					
S_fume mixes	S_fume_5, 10, 15 with silica fume % = 5, 10, and 15; w/cm = 0.45					

Table 2: Chemical composition of the cement and SCM based on manufacturer's mill cert.

Chemical compound (%)	Type I/II cement	Class F fly ash	GGBFS	Silica fume
SiO_2	21.3	56.50	32.00	92.86
Al_2O_3	3.20	23.70	12.90	Not listed
Fe_2O_3	2.90	3.60	0.50	Not listed
SO_3	3.10	0.20	3.70	0.33
CaO	64.30	9.20	41.2	Not listed
MgO	2.10	1.00	5.70	Not listed
Na_2O	0.26	0.29	0.21	0.20
K_2O	0.42	0.22	0.41	0.70
Loss on ignition	1.35	0.62	1.40	3.33
Blaine fineness (m^2/kg)	391	NA*	480	21,910
Specific gravity	3.10	2.05	2.87	2.26

*Fineness of fly ash was 26.6 percent of retained on 45 μm (no. 325) standard sieve. Blaine fineness was not available.

was cast and kept in sealed conditions in a plastic mold for electrical conductivity measurements. Electrical conductivity was measured using one embedded time-domain reflectometry (TDR) sensor, Type 5TE from Meter Group [23]. The 5TE sensor was used to measure T and electrical conductivity (σ) of the mortar. The sensor applies an electrical current to and measures the resistivity of the medium between the sensor probes. This type of sensor is currently used in soil applications for the assessment of soil salinity and water content. The authors demonstrated the application of the sensors in cement-based materials in earlier publications [6, 7]. In this study, one 5TE sensor was vertically embedded at middepth location of each cylinder specimen during casting. All sensors were connected to a CR1000 datalogger from Campbell Scientific, and the sensor data were recorded in 5-minute intervals. Specimens were covered at the top with double plastic bags during the first 24 hours. After this initial period, while the specimens were kept in their molds, the plastic bags were removed, and the tops were sealed using adhesive aluminum tape. Specimens were kept in the sealed condition in the laboratory with controlled ambient temperature at 21°C for 11–13 months.

2.3. Temperature Regimes. The specimens were placed in a temperature-controlled chamber and were subjected to stepwise temperature change, T_c's: 5, 10, 15, 23, 30, 40, and 50°C. Each T_c was kept constant for approximately five days until the sensor-based measurements of T and σ exhibited minimal fluctuations (standard deviation of $T < 0.1$°C and standard deviation of $\sigma < 0.005$ dS/m). The temperature regime based on the sensor in mix W0.35 is provided in Figure 1 as an example.

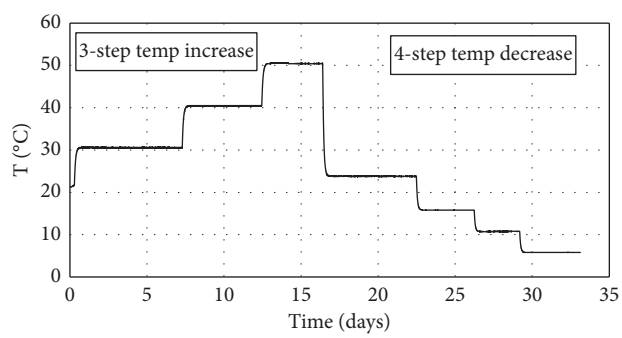

Figure 1: Stepwise temperature regime during the experiment obtained from the sensor at midlocation of mix W0.35.

3. Results and Data Analysis

3.1. Effect of Temperature on Electrical Conductivity of Mix Groups. Figure 2 presents the changes in σ as a function of T for all the tested mixtures. Each data point is the average of all of σ and T data during one T_c step. As seen in Figure 2, σ increases as temperature is increased for all the tested mixtures. This trend is expected, since the increase in T is associated with increased mobility of ions in the pore solution, resulting in higher conductivity [14]. At $T_c > 23$°C, σ increases at a faster rate with the same incremental increase in temperature (exponential T-σ trend.) Therefore, $T_c = 23$°C is used as the reference temperature in the following sections.

The effect of mixture parameters can be identified based on the difference in the values of σ among the different mixtures in Figure 2(a); mixtures with lower w/cm exhibit

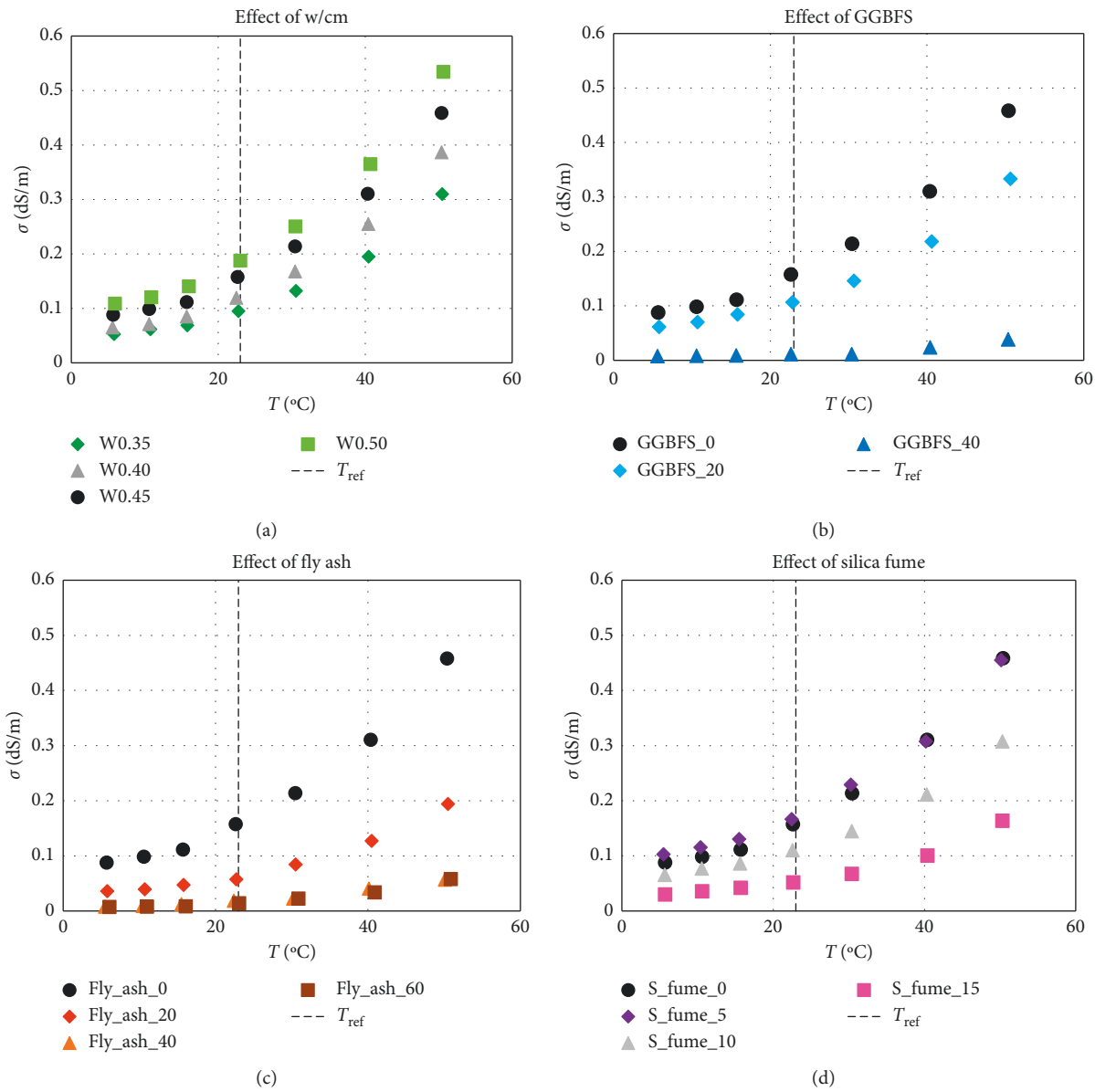

Figure 2: Changes in σ with T for mixes varying in (a) w/cm, (b) GGBFS, (c) fly ash, and (d) silica fume.

lower values of σ, as an effect of lower amount of pore solution in the pore system, as well as less connected (more tortuous) capillary pores [6, 24, 25]. In Figures 2(b)–2(d), the use of SCM results in overall lower values of σ compared to the plain mixture and the more use of SCM results in lower values of conductivity. The trend is due to the products of SCM late pozzolanic reaction, which fills the capillary pores, making the pore system discontinuous and less conductive [6, 26, 27]. At $T_c < 23^\circ$C, σ data of GGBFS_40, Fly_ash_40, and Fly_ash_60 approach near-zero values. Since the accuracy of 5TE sensors is 0.01 dS/m, the absolute values of σ may not be reliable for these sensors.

3.2. Linear Temperature Correction (LTC). Linear temperature correction (equation 1) was applied to the experimental T-σ data shown in Figure 3. The effective conductivity at $T_c = 23^\circ$C is marked as σ_{ref}. Figure 3 presents the σ/σ_{ref} ratio at various T_c based on the experimental data and the fitted LTC for all the mixtures. The calibrated values of coefficient α were determined using the Solver function in Microsoft Excel, such that the sum of the squared differences between the measured and corrected σ/σ_{ref} is minimized. Table 3 shows the calibrated α values and high coefficients of determination ($R^2 > 0.81$) for the fitted lines. However, for several mixtures, LTC results in negative σ values for $T_c = 5^\circ$C, which bears no physical meaning and should be assumed as zero. Also, the values of α obtained in this study are higher than those for concrete reported by Weiss et al., ranging from 1.87–3.37%/°C [17]. The temperature range in [17] was 5–30°C, compared to 5–50°C in this study. The higher T_c, results in a steeper exponential σ-T correlation, therefore LTC produces suboptimal fit to the data. The

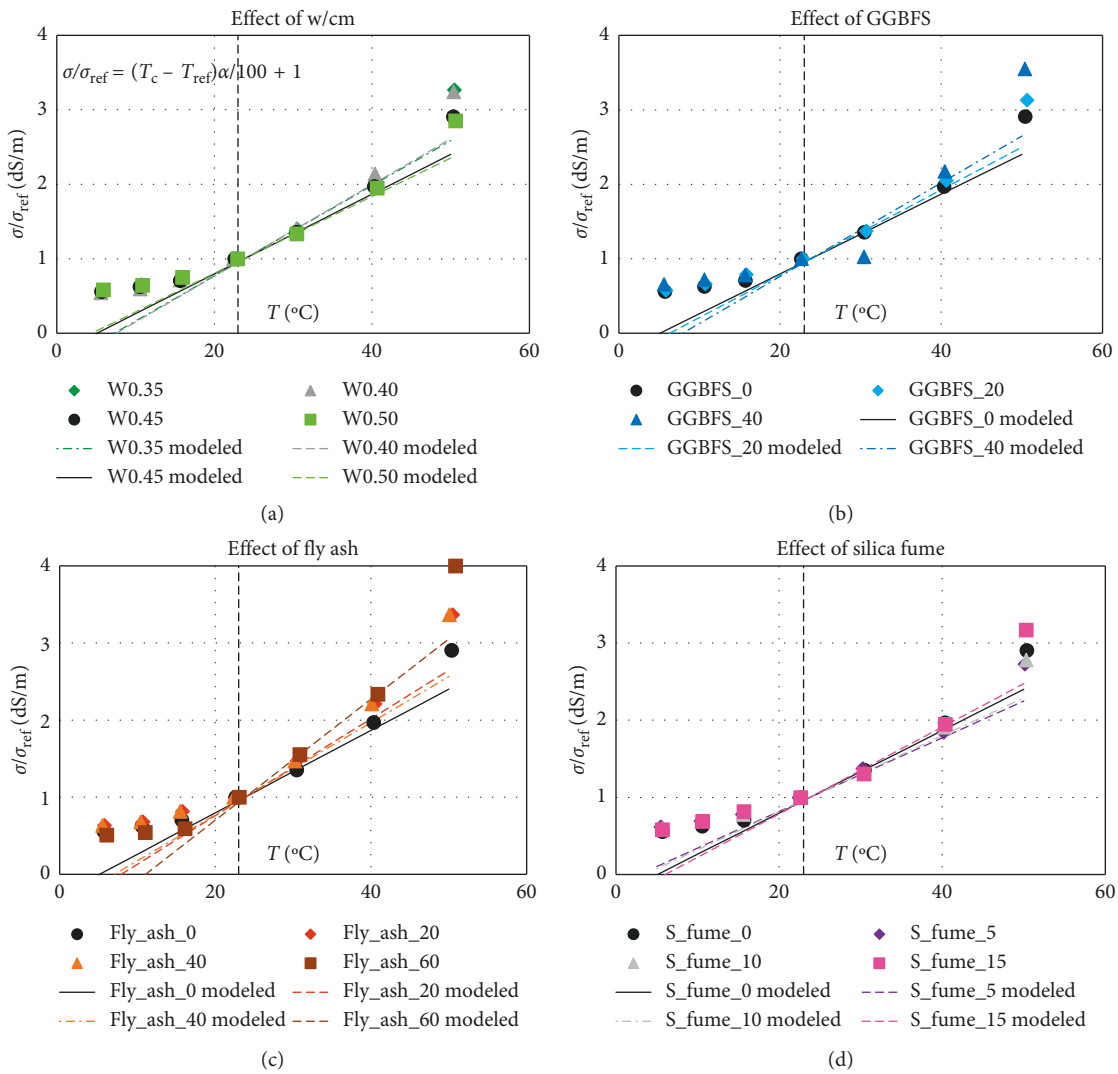

Figure 3: Experimental and modeled σ/σ_{ref} at various T_c based on LTC (equation 1) for all mixtures. Vertical dashed line marks $T_{ref} = 23^{\circ}C$.

Table 3: Calibrated values of coefficient α in LTC (equation 1) for all tested mixtures and values of R^2.

Mix. ID	W0.35	W0.40	W0.45	W0.50	GGBFS_20	GGBFS_40
α [%/°C]	6.06	6.15	5.35	5.16	5.72	6.29
R^2	0.85	0.87	0.89	0.88	0.85	0.90
Mix. ID	Fly_ash_20	Fly_ash_40	Fly_ash_60	S_fume_5	S_fume_10	S_fume_15
α [%/°C]	6.28	5.97	7.83	4.77	4.93	5.63
R^2	0.81	0.91	0.83	0.87	0.87	0.83

temperature range of 5–30°C seems to be the optimum range for the LTC model. To address this limitation, different temperature corrections are evaluated in Sections 3.3. and 3.4.

3.3. New Bilinear Temperature Correction (BLTC). Based on the results in Figure 3, the rate of change in σ with T_c is different above and below the reference temperature. Therefore, a bilinear temperature correction (BLTC) model is proposed here, with two individual temperature coefficients (α_1 and α_2) for the ranges below and above T_{ref}:

$$\frac{\sigma}{\sigma_{ref}} = \left\{ \begin{array}{ll} \dfrac{(T_c - T_{ref})\alpha_1}{100} + 1, & \text{for } T_c < T_{ref} \\ \dfrac{(T_c - T_{ref})\alpha_2}{100} + 1, & \text{for } T_c > T_{ref} \end{array} \right\}. \quad (3)$$

Values of α_1 and α_2 for each mixture were determined using the Microsoft Excel Solver functions as described in Section 3.2. The calibrated coefficients α_1 and α_2, with the corresponding R^2 values for BLTC are listed in Table 4. The experimental data and the new model are plotted versus T_c in Figure 4. As seen in Table 4, the new model provides a better fit to the data compared

Table 4: Calibrated values α_1 and α_2 BLTC (equation 3) for all tested mixtures and R^2 values.

Mix. ID	W0.35	W0.40	W0.45	W0.50	GGBFS_20	GGBFS_40
α_1 (%/°C)	2.84	3.06	2.92	2.72	2.64	2.22
α_2 (%/°C)	7.41	7.39	6.36	6.21	7.02	8.01
R^2	0.97	0.98	0.98	0.98	0.98	0.97
Mix. ID	Fly_ash_20	Fly_ash_20	Fly_ash_60	S_fume_5	S_fume_10	S_fume_15
α_1 (%/°C)	2.35	3.77	3.44	2.44	2.50	2.51
α_2 (%/°C)	7.92	6.89	9.69	5.75	5.95	6.95
R^2	0.98	0.97	0.97	0.98	0.98	0.96

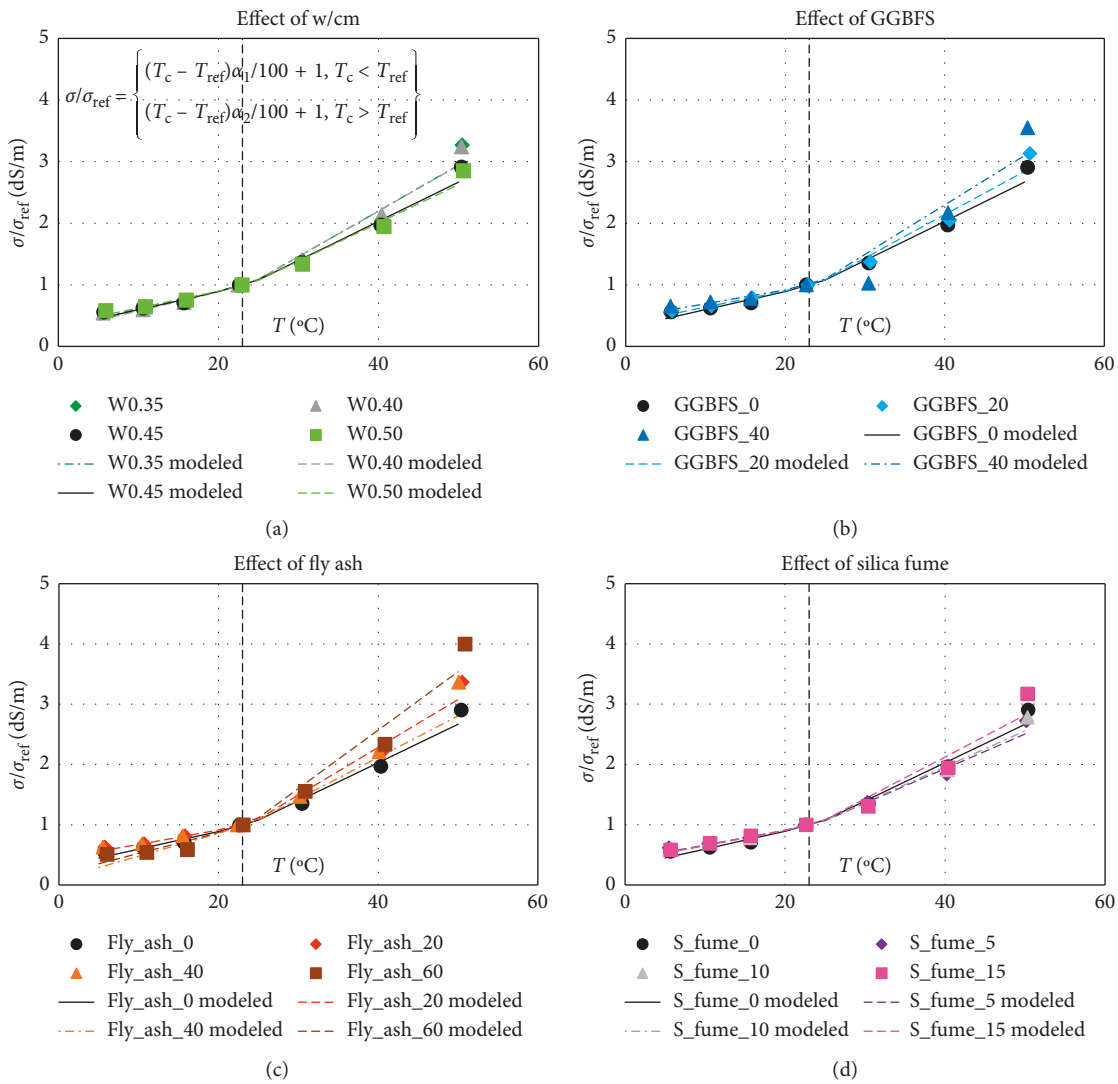

Figure 4: Experimental and modeled σ/σ_{ref} at various T_c's based on bilinear temperature correction (equation 3) for all mixtures. Vertical dashed line corresponds to T_{ref} = 23°C.

to the LTC (Table 3) ($R^2 > 0.96$.) The fitted values for the coefficients α_2 are higher than the α_1 values, indicating higher temperature sensitivity when $T_c > T_{ref}$. Calibrated values of α_1 are within the range identified by Weiss et al.; however, values of α_2 surpass the 1.87–3.37%/°C range due to higher T_c used in this study [17]. With a better fit to the data, the new BLTC model presents a promising alternative to LTC for a wide range of temperature.

3.4. Arrhenius Temperature Correction (ATC). Temperature correction based on E_c, defined earlier in equation 2 as ATC, was applied to the experimental σ-T data. Optimal values of E_c for each mixture are provided in Table 5 with the corresponding R^2. Figure 5 presents the experimental σ/σ_{ref} data and the fitted ATC model for all mixtures. As seen in Table 5, ATC provides a better fit to the data compared to the LTC and BLTC methods ($R^2 > 0.98$). The

Table 5: Optimized values of E_c for all tested mixtures and the coefficient of determination (R^2).

Mix. ID	W0.35	W0.40	W0.45	W0.50	GGBFS_20	GGBFS_40
E_c (kJ/mol)	33.40	33.17	30.26	29.80	32.18	35.26
R^2	0.99	1.00	1.00	1.00	0.99	0.98
Mix. ID	Fly_ash_20	Fly_ash_40	Fly_ash_60	S_fume_5	S_fume_10	S_fume_15
E_c (kJ/mol)	34.49	32.05	39.34	28.15	28.86	32.13
R^2	0.99	0.99	0.99	0.99	0.99	0.98

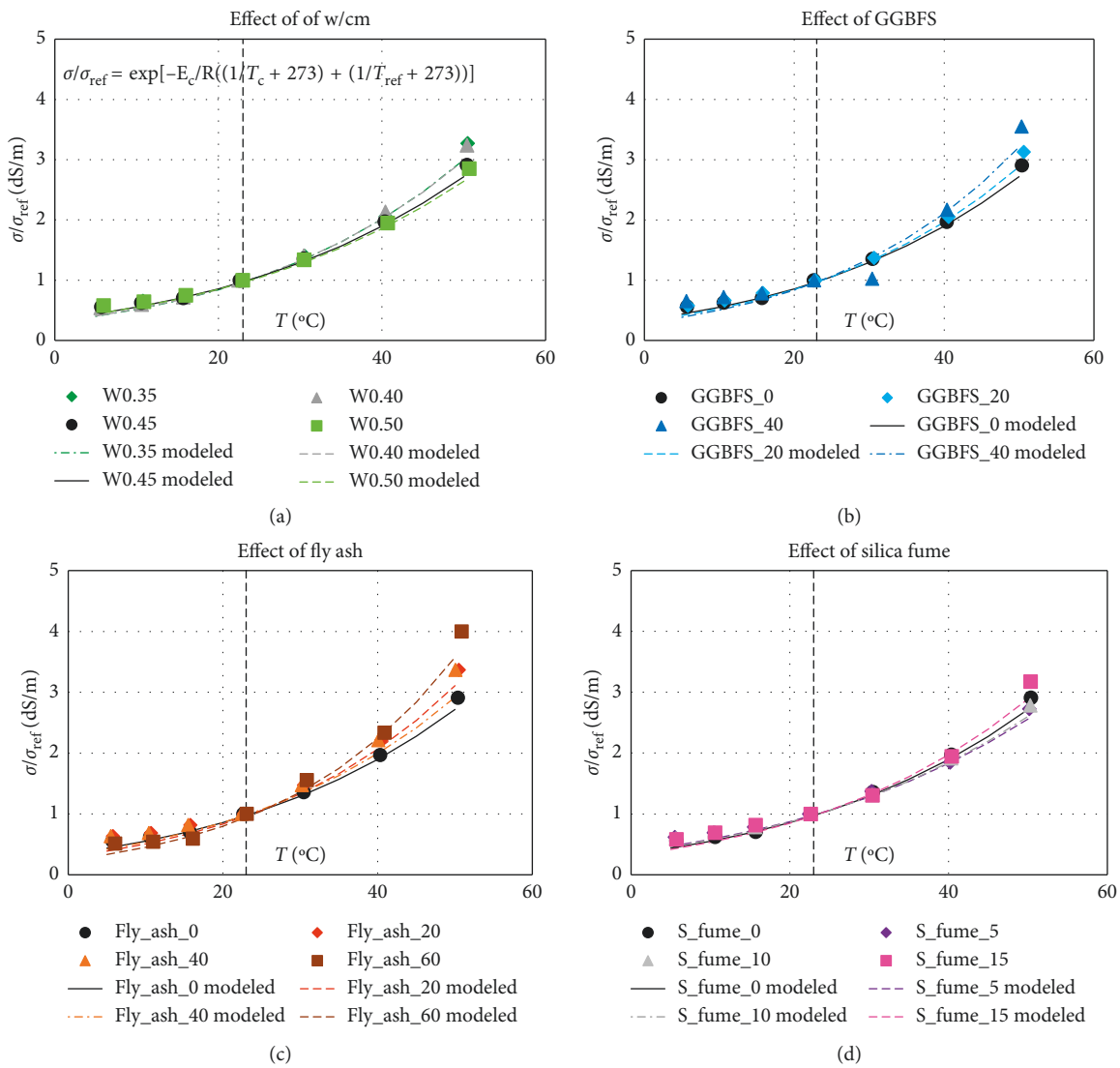

Figure 5: Experimental and modeled σ/σ_{ref} at various T_c based on ATC (equation 2) for all mixtures. Vertical dashed line corresponds to T_{ref} = 23°C.

values of E_c fall in the 23.4 to 42.47 kJ/mol range, which is reported for sealed concrete in the literature [3, 8, 17].

3.5. Effect of Mixture Design on Temperature Sensitivity. The temperature sensitivity of σ measurements for each mixture can be inferred from the values of the correction coefficients (α and E_c), listed previously in Tables 3–5. Based on the obtained results, higher w/cm decreases the sensitivity of σ of the mix to temperature. This trend is consistent with findings of Weiss et al., who reported lower temperature sensitivity of specimens at higher degree of saturation [17]. It is possible that the diluted pore solution of mixtures with higher w/cm exhibits less increase in ionic mobility at elevated temperatures. Mixtures with SCM generally exhibit higher sensitivity to temperature correction compared to the control mix; the only exceptions are S_fume_5 and S_fume_10. It is likely that the differences in temperature

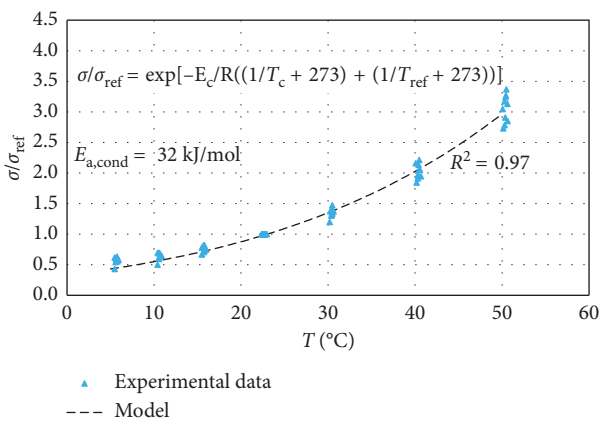

Figure 6: A single ATC for all tested mixtures based on $E_{a,cond}$.

sensitivity are due to the differences in pore solution alkalinity and chemical composition. It is also noteworthy that Fly_ash_60 and GGBFS_40 have the highest values of E_c due to low σ at $T_c = 5^\circ$C. The value of σ at this low temperature is close to the sensor's limit of sensitivity so if the two mixtures are removed from the data, the values of E_c are within a relatively narrow range for all mixtures (maximum difference among E_c values is 18%). It is therefore beneficial to determine a single average value of E_c for all mixtures as shown in Figure 6. The calibrated value of E_c is 32 kJ/mol, and the fit is satisfactory ($R^2 = 0.97$).

4. Conclusions

An experimental study was conducted with the primary objective to evaluate existing temperature correction methods for electrical conductivity (σ) of concrete. Twelve mortar mixtures were kept in stepwise temperature change in 5–50°C range. Three methods of linear, bilinear, and Arrhenius temperature correction (LTC, BLTC, and ATC) were evaluated. Results revealed that LTC gives acceptable fit to the experimental data only for the temperatures up to 30°C. Bilinear temperature correction, with different coefficients below and above the reference temperature of 23°C, presented a favorable alternative to linear correction. Lastly, ATC provided the best fit among all methods over the full temperature range. Comparison of different mixtures indicated that increase in water-to-cementitious ratio yields lower temperature sensitivity. The implementation of supplementary cementitious materials generally increased the responsiveness of σ to the temperature change. As the values of temperature correction coefficients did not vary substantially among the tested mixtures, a single E_c at 32 kJ/mol is recommended for all tested mixtures. Future research will include a wider range of mixture designs and evaluation of the established corrections for different electrical methods, such as axial and surface resistivity meters.

Data Availability

The temperature-conductivity data used to support the findings of this study are available from the corresponding author upon request.

Conflicts of Interest

The authors declare that there are no conflicts of interest.

Acknowledgments

Funding was provided by Portland Cement Association fellowship award. The authors acknowledge Meter Group for providing the instrumentation and technical support for this study. Premix Pullman is acknowledged for aggregate donation. Thanks to Ash Grove Cement Company for supplying cement, Lafarge for fly ash and slag, and BASF for silica fume.

References

[1] H. Layssi, P. Ghods, A. R. Alizadeh, and M. Salehi, "Electrical resistivity of concrete," *Concrete International*, vol. 37, no. 5, pp. 41–46, 2015.

[2] L. Xiao and Z. Li, "Early-age hydration of fresh concrete monitored by non-contact electrical resistivity measurement," *Cement and Concrete Research*, vol. 38, no. 3, pp. 312–319, 2008.

[3] R. Spragg, C. Villani, K. Snyder, D. Bentz, J. W. Bullard, and J. Weiss, "Factors that influence electrical resistivity measurements in cementitious systems," *Transportation Research Record: Journal of the Transportation Research Board*, vol. 2342, no. 1, pp. 90–98, 2013.

[4] J. Chen, Z. Li, and X. Jin, "Critical features of microstructure development of early-age cement paste revealed by non-contact electrical resistivity measurement," *Construction and Building Materials*, vol. 154, pp. 1121–1129, 2017.

[5] K. B. Sanish, N. Neithalath, and M. Santhanam, "Monitoring the evolution of material structure in cement pastes and concretes using electrical property measurements," *Construction and Building Materials*, vol. 49, pp. 288–297, 2013.

[6] M. Rangelov and S. Nassiri, "Empirical time-dependent tortuosity relations for hydrating mortar mixtures based on modified Archie's law," *Construction and Building Materials*, vol. 171, pp. 825–838, 2018.

[7] M. Rangelov and S. Nassiri, "Sensor-based time-dependent formation factor in prediction of chloride ingress in mortar," *Magazine of Concrete Research*, pp. 1–38, 2018.

[8] Y. A. Villagrán Zaccardi, J. Fullea García, P. Huélamo, and Á. A. Di Maio, "Influence of temperature and humidity on Portland cement mortar resistivity monitored with inner sensors," *Materials and Corrosion*, vol. 60, no. 4, pp. 294–299, 2009.

[9] Z. Liu, Y. Zhang, and Q. Jiang, "Continuous tracking of the relationship between resistivity and pore structure of cement pastes," *Construction and Building Materials*, vol. 53, pp. 26–31, 2014.

[10] M. R. Nokken and R. D. Hooton, "Using pore parameters to estimate permeability or conductivity of concrete," *Materials and Structures*, vol. 41, no. 1, pp. 1–16, 2007.

[11] T. D. Rupnow and P. J. Icenogle, "Surface resistivity measurements evaluated as alternative to rapid chloride permeability test for quality assurance and acceptance," *Transportation Research Record: Journal of the Transportation Research Board*, vol. 2290, no. 1, pp. 30–37, 2012.

[12] W. J. Weiss, R. P. Spragg, O. B. Isgor, M. T. Ley, and T. Van Dam, "Toward performance specifications for concrete: linking resistivity, RCPT and diffusion predictions using

the formation factor for use in specifications," in *High Tech Concrete: Where Technology and Engineering Meet*, pp. 2057–2065, Springer, Cham, Switzerland, 2018.

[13] P. J. Tumidajski and A. S. Schumacher, "On the relationship between the formation factor and propan-2-ol diffusivity in mortars," *Cement and Concrete Research*, vol. 26, no. 9, pp. 1301–1306, 1996.

[14] P. Azarsa and R. Gupta, "Electrical resistivity of concrete for durability evaluation: a review," *Advances in Materials Science and Engineering*, vol. 2017, Article ID 8453095, 30 pages, 2017.

[15] S. W. Tang, X. H. Cai, Z. He et al., "The review of pore structure evaluation in cementitious materials by electrical methods," *Construction and Building Materials*, vol. 117, pp. 273–284, 2016.

[16] R. Spragg, C. Villani, and J. Weiss, "Electrical properties of cementitious systems: formation factor determination and the influence of conditioning procedures," *Advances in Civil Engineering Materials*, vol. 5, no. 1, pp. 124–148, 2016.

[17] J. Weiss, A. Amirkhanian, P. Suraneni, R. Spragg, and A. Coyle, "Comparison of linear temperature corrections and activation energy temperature corrections for electrical resistivity measurements of concrete," *Advances in Civil Engineering Materials*, vol. 7, no. 1, pp. 174–187, 2018.

[18] W. J. McCarter, T. M. Chrisp, G. Starrs, P. A. M. Basheer, and J. Blewett, "Field monitoring of electrical conductivity of cover-zone concrete," *Cement and Concrete Composites*, vol. 27, no. 7-8, pp. 809–817, 2005.

[19] R. B. Polder, "Test methods for on site measurement of resistivity of concrete - a RILEM TC-154 technical recommendation," *Construction and Building Materials*, vol. 15, no. 2-3, pp. 125–131, 2001.

[20] T. M. Chrisp, G. Starrs, W. J. McCarter, E. Rouchotas, and J. Blewett, "Temperature-conductivity relationships for concrete: an activation energy approach," *Journal of Materials Science Letters*, vol. 20, no. 12, pp. 1085–1087, 2001.

[21] W. J. McCarter, "Effects of temperature on conduction and polarization in Portland cement mortar," *Journal of the American Ceramic Society*, vol. 78, no. 2, pp. 411–415, 1995.

[22] ASTM C305/C305-14, 2014, *Standard Practice for Mechanical Mixing of Hydraulic Cement Pastes and Mortars of Plastic Consistency*, ASTM International, West Conshohocken, PA, USA, 2014.

[23] Meter Group, *ECH$_2$O 5TE Soil Moisture, Temperature, and Electrical Conductivity Sensor*, 2018, https://www.metergroup.com/environment/products/ech2o-5te-electrical-conductivity/.

[24] J. Weiss, T. J. Barrett, C. Qiao, and H. Todak, "Toward a specification for transport properties of concrete based on the formation factor of a sealed specimen," *Advances in Civil Engineering Materials*, vol. 5, no. 1, pp. 179–194, 2016.

[25] X. Chen and S. Wu, "Influence of water-to-cement ratio and curing period on pore structure of cement mortar," *Construction and Building Materials*, vol. 38, pp. 804–812, 2013.

[26] B. Lothenbach, K. Scrivener, and R. D. Hooton, "Supplementary cementitious materials," *Cement and Concrete Research*, vol. 41, no. 12, pp. 1244–1256, 2011.

[27] M. C. G. Juenger and R. Siddique, "Recent advances in understanding the role of supplementary cementitious materials in concrete," *Cement and Concrete Research*, vol. 78, pp. 71–80, 2015.